AGU PUBLICATIONS

Geophysical Research Letters

RESEARCH LETTER
10.1002/2015GL066916

The imprint of climate and geology on the residence times of groundwater

Reed M Maxwell[1], Laura E Condon[1], Stefan J Kollet[2], Kate Maher[3], Roy Haggerty[4], and Mary Michael Forrester[1]

[1]Hydrologic Science and Engineering Program, Integrated GroundWater Modeling Center, Department of Geology and Geological Engineering, Colorado School of Mines, Golden, Colorado, USA, [2]Centre for High-Performance Scientific Computing in Terrestrial Systems, Institute for Bio- and Geosciences, Agrosphere (IBG-3), Research Centre Jülich, Jülich, Germany, [3]Department of Geological Sciences, Stanford University, Stanford, California, USA, [4]College of Earth, Ocean and Atmospheric Sciences, Oregon State University, Corvallis, Oregon, USA

Key Points:
- We can model the residence times of groundwater at continental scales
- The peak residence times correlate with hydraulic conductivity
- The variance of residence time correlates with potential recharge

Supporting Information:
- Texts S1 and S2, Table S1, and Figure S1

Correspondence to:
R. M. Maxwell,
rmaxwell@mines.edu

Citation:
Maxwell, R. M., L. E. Condon, S. J. Kollet, K. Maher, R. Haggerty, and M. M. Forrester (2016), The imprint of climate and geology on the residence times of groundwater, *Geophys. Res. Lett.*, *43*, 701–708, doi:10.1002/2015GL066916.

Received 6 NOV 2015
Accepted 11 DEC 2015
Accepted article online 16 DEC 2015
Published online 29 JAN 2016

Abstract Surface and subsurface flow dynamics govern residence time or water age until discharge, which is a key metric of storage and water availability for human use and ecosystem function. Although observations in small catchments have shown a fractal distribution of ages, residence times are difficult to directly quantify or measure in large basins. Here we use a simulation of major watersheds across North America to compute distributions of residence times. This simulation results in peak ages from 1.5 to 10.5 years, in agreement with isotopic observations from bomb-derived radioisotopes, and a wide range of residence times—from 0.1 to 10,000 years. This simulation suggests that peak residence times are controlled by the mean hydraulic conductivity, a function of the prevailing geology. The shape of the residence time distribution is dependent on aridity, which in turn determines water table depth and the frequency of shorter flow paths. These model results underscore the need for additional studies to characterize water ages in larger systems.

1. Introduction

The residence time of water in the subsurface dictates contaminant concentrations [*Sposito and Jury*, 1988; *Quinodoz and Valocchi*, 1993], determines the supply of nutrients to aquatic ecosystems [*Laudon et al.*, 2011; *Flewelling et al.*, 2012], and moderates the conversion of rock to solute [*Maher and Chamberlain*, 2014]. Nevertheless, the distribution of water ages in large river basins remains poorly quantified [*Kirchner*, 2003; *McDonnell et al.*, 2010; *Rinaldo et al.*, 2011]. Challenges in measuring water ages, the inability of simple models to predict residence times across multiple spatial scales, and limitations in the scale over which numerical simulations can be applied, have long posed a barrier to quantifying the residence time distributions for groundwater discharging into rivers in large-scale (100–1000 km^2) watersheds.

Connections between topography and hydrology have been studied for decades [*Tóth*, 1963; *Montgomery and Dietrich*, 1992], yet open questions remain about the topographic influences on the quantity, movement, distribution, and spatiotemporal organization of groundwater residence times at the continental scale [*McDonnell et al.*, 2010]. For example, many traditional models that represent transport using exponential or advection-dispersion frameworks inadequately describe the fractal behavior of watershed-scale residence time distributions [*Kirchner et al.*, 2000; *Haggerty et al.*, 2002; *Scher et al.*, 2002; *Stonedahl et al.*, 2012; *Kirchner and Neal*, 2013]. The inability of traditional models to capture fractal scaling in residence time distributions suggests that conventional hydrologic residence time theories are missing the majority of old water [*Botter et al.*, 2010; *Frisbee et al.*, 2013; *Hrachowitz et al.*, 2013].

Fractal residence time distributions have been attributed to a number of factors, including geology, topography, and chemical reactions that impact tracers; however, a growing body of literature attributes this fractal behavior to fractal topography, rather than subsurface heterogeneity [*McGuire et al.*, 2005; *Cardenas*, 2007; *Cardenas*, 2008; *Kollet and Maxwell*, 2008]. Although heterogeneity in hydraulic conductivity can amplify the fractal signal in residence time distributions [*Cardenas*, 2007; *Fiori and Russo*, 2008; *Jiang et al.*, 2010], heterogeneity is not necessary to induce fractal behavior. In fact, simple water-table geometries in homogeneous materials can exhibit this type of residence time distribution [*Cardenas et al.*, 2008]. Correlations have been observed between median flow path length and gradient at one site [*McGuire et al.*, 2005]; still, quantifying the drivers of residence time at large spatial scales remains an important research topic.

Understanding the large-scale drivers of the peak and spread in residence time distributions has important implications for the predictability of hydrologic transport. Yet, few studies address connections between catchment residence times and topographic, climatic, and subsurface characteristics at the continental scale, as noted by *Tetzlaff et al*. [2009]. Those that do, demonstrate that steeper montane regions exhibit shorter residence times, whereas subdued terrain has less of an influence on flow regimes [*Wörman et al*., 2007]. *Wörman et al*. [2007] also showed that geomorphically varied regions display similar residence time distributions and large-scale topographic features tend to determine fluxes along deep subsurface flow paths. Here we expand on prior large-scale analyses, which relied on topographic transforms to define groundwater configuration, by explicitly simulating the groundwater system using physically based equations. This approach allows for the direct simulation of ages driven by topography, geology (hydraulic conductivity), and climate (aridity) over a continental domain.

2. Methods

A Lagrangian particle-tracking technique was applied to trace streamlines from each river cell through groundwater and the unsaturated zone to the recharge location with a steady-state, integrated simulation of surface and subsurface flow using ParFlow over a 6.3×10^6 km^2 domain published previously [*Maxwell et al*., 2015]. The flow simulation is well documented and the results were previously compared to a large number of observations (>160,000 groundwater and >4000 surface water). The model domain extends 102 m below ground surface (following the terrain), using a 1 km lateral resolution and variable vertical resolution. Complete model input parameters are provided in *Maxwell et al*. [2015] and in section 1 of the supporting information and are briefly summarized here. The upper 2 m of the subsurface is soil with material properties assigned based on soil texture [*Schaap and Leij*, 1998]; for the deeper 100 m properties were assigned based on lithology modified from *Gleeson et al*. [2011] to reduce the variability of hydraulic conductivity and to include a slope-based empirical approach to better represent basin-and-range formation [*Fan et al*., 2007]. Using this approach, with large grid cells, both the range of effective hydraulic conductivities (0.005 to 0.1 m/h) and porosities (0.1–0.3) are lower than point observations. It was run to steady state using a modern (1950–2000) estimate of spatially distributed precipitation minus evapotranspiration (*P-ET*). The flow simulation employed no-flow boundary conditions on the bottom of the domain. This boundary condition may bias the simulation by under representing longer travel times; however, this is a necessary simplification given the limited data on depth to low hydraulic conductivity bedrock at the continental scale.

In order to simulate the total subsurface residence time from ground surface to river (i.e., the water age at the river discharge), two particles were assigned randomly at each of the river cells within this flow model; flow velocities were reversed and particles were traced *backward* from the streambed through groundwater back to the point of recharge. The particle simulations were run after the flow model (using two separate simulations) and each particle is run until the recharge point is reached resulting in a unique total simulation time for every particle in the simulation. This approach focused particles at the endpoint of interest (the river) and resulted in 4.14×10^6 total particles, providing a balance between computation efficiency and resolution. This method is identical to a particle tracking process used previously in a much smaller watershed [*Kollet and Maxwell*, 2008].

Although the simulation presented here is the first continental scale analysis of groundwater residence times using an integrated model, there are some important limitations to note. Due to the modern estimates of *P-ET* and relatively shallow domain, this approach does not account for deeper water, such as is present deeper than 102 m (particularly true in deeper, alluvial systems) or recharged under a different climate regime. Similarly, the Great Lakes are present in the domain but are not included in the analysis because lake processes are not explicitly simulated. This simulation also cannot directly capture event-type flow or topography at less than the 1 km lateral resolution of the domain, which is important to capture regions of convergence near streams. Uncertainties are present in the subsurface inputs, particularly effective hydraulic conductivities and fracture porosities at large scales. Finally, the approach used here omits anthropogenic influences on flow, such as groundwater pumping, irrigation, and surface water diversions and management. Thus, the simulation is representative of modern climate mean flow; ages and simulated residence times greater than 10,000 years should be viewed as less certain. We recognize the uncertainty in the current subsurface data set and modeling assumptions. Although we could not do a comprehensive sensitivity analysis given the computational demands (as noted in *Maxwell et al*. [2015], the flow simulation upon which this particle tracking is based took approximately 2.5 M core hours), our results suggest that better understanding model inputs such as the depth of bedrock, subsurface properties such as hydraulic conductivity and porosity and finer representations of topography may improve flow simulations.

All surface water travel times were calculated in addition to the groundwater residence times. The peak travel times were roughly 100 h for all basins and the oldest surface water age was 62 days. Because the time spent in surface water is small compared to the time spent in the unsaturated zone and in the groundwater, the ages can be compiled for the entire domain and for each basin without adding surface water travel times. The point values of age were mapped to regular grids with 1 km and 10 km cell sizes over the model domain using log means of residence time. Histograms of age were generated using the *R* software package and each particle was flux weighted by its corresponding *P-ET* value.

3. Results and Discussion

Figure 1 shows the residence time distribution that results from tracking particles from every river cell, through the groundwater and vadose zone, to their recharge locations based upon the simulated three-dimensional surface and subsurface flow velocity field. Although basins viewed at large scales may appear to be composed of primarily older water, the inset of the upper Colorado headwaters (Figure 1b) demonstrates the juxtaposition of very old and very young water.

Because the transit time in the river network is much smaller than in the subsurface, these distributions represent both a probability density function of the ages of water discharged from the mouth of the river network and the breakthrough curve of a unit concentration tracer initiated across the land surface. Figure 2 shows the mass fraction versus arrival time at the ground surface for the entire domain (a) and for major river basins (b–g) shown in Figure 1, or equivalently, the distribution of residence times from the point of recharge at the ground surface to the surface water discharge point. Resulting peak stream water ages range from 1.5 to 10.5 years depending on the basin. However, quantities of both very young (0.1 year) and very old (10,000 years) water are also present in all watersheds. Similar to studies of water residence time in smaller-scale basins [*Kirchner et al*., 2000; *Haggerty et al*., 2002; *Kirchner and Neal*, 2013], these distributions are all heavy tailed (see discussion of Figure 3, below), exhibit power-law scaling over some range and often have a departure at late time. The Colorado and Snake River systems have slightly bimodal age distributions (Figures 2b and 2d), a novel result likely resulting from focused recharge at higher elevation headwaters composed of fractured bedrock and lower-recharge alluvium in the valleys and multi-scale, or nested Tòthian flow systems [*Cardenas*, 2007]. The peak ages predicted by the model agree well with several estimated, effective ages inferred from tritium (^{3}H) concentrations (as compiled in *Stewart et al*. [2010]). As shown on Figures 2b, 2c, 2e, and 2f, ages for the Upper Mississippi of 10 ± 3 years from observations are in agreement with the calculated 10 year peak arrival; ages 10 ± 3 years observed for the Ohio agree with simulations of 7.5 years; and 4 years observed for the Missouri agree with simulated ages of 3.5 years. Note that these observed ages correspond to estimated groundwater contributions and not shorter surface water residence times. The Colorado simulated peak age of 2 years is somewhat less than the inferred age of 14.3 years; however, the simulation suggests a bimodal distribution with peaks centered around both 2 and 100 years (Figure 2b). However, given the 102 m depth of the model, deeper flow paths that could shift the second 100 year peak to older values are not included in these distributions.

Figure 3 plots the log power spectra for the residence time distributions shown in Figure 2 with the major basins shown (Figures 3b–3g) as well as the entire domain (Figure 3a). In this figure, the uncorrelated white noise apparent at high frequencies corresponds to times prior to the peak ages in Figure 2 (for reference the histogram peak times are denoted with the lighter dashed lines on Figure 3). The noisy behavior for ages less than the peak is a function of the shape of the breakthrough curves in Figure 2 and the lateral resolution of the domain. A higher resolution model would facilitate the simulation of shorter flow paths and could decrease the peak ages in Figure 2 [*Haggerty et al*., 2002]. Beyond periods of 10,000 years we see a leveling off and eventually small decreases in the power spectra in all basins. This is likely due to a decrease in particle resolution for very long flow paths. However, given the physical modeling setup, which omits deeper groundwater flow paths and water recharged under prior climates, we would expect these spectra to be less certain. Between periods of 10 and 10,000 years, clear scaling, as demonstrated by monotonically increasing power as

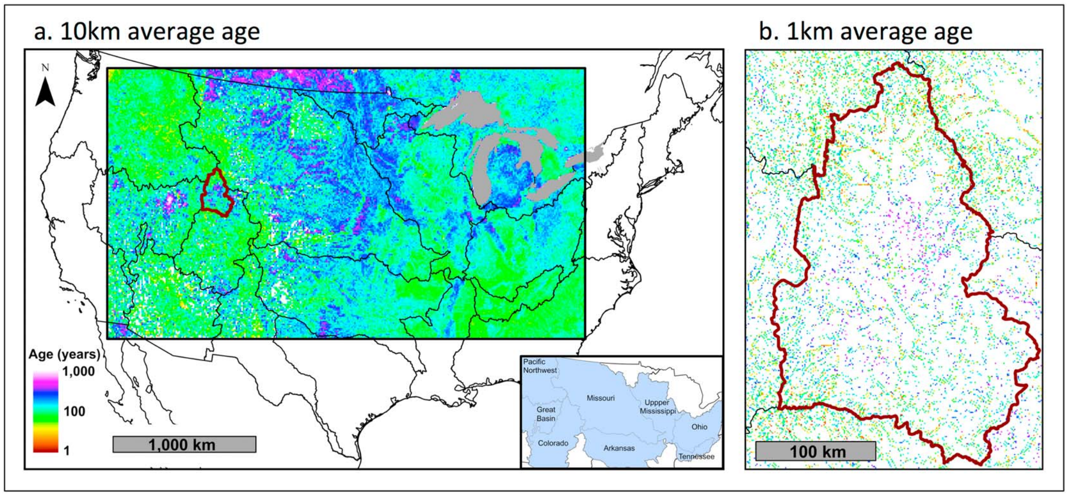

Figure 1. A spatial map of groundwater residence times for the entire domain, as calculated from river to recharge locations, demonstrates the wide range of ages resulting from this simulation. The point ages derived from the backward particle trajectories are (a) averaged to a 10 km pixel resolution over the model domain and (b) zoomed-in over the Upper Colorado at a 1 km pixel resolution. Note that the Great Lakes (grayed out) are not included in this simulation.

a function of period, is evident in all basins. The overall log slope for these regions is slightly greater than unity, yet distinct breaks appear in most basins. The Colorado and Pacific NW show the most consistent scaling.

The relationships among age distributions and observable properties provide insight into the processes that govern residence time. Prior studies have shown that fractal topography generates heavy-tailed age distributions [*Wörman et al*., 2007]. The architecture of the subsurface, expressed via hydraulic conductivity (K) and porosity, and the prevailing climate, expressed via aridity, also play a critical role in determining age. When the peak ages (Figures 2b–2g) are plotted as a function of average ln(K) (in m/d) averaged over each of the basins (Figure 1), the resulting pattern suggests a dependence on the basin-averaged hydraulic conductivity, indicating that soil and rock type may influence peak age (Figure 4a) at continental scales. This relationship is likely

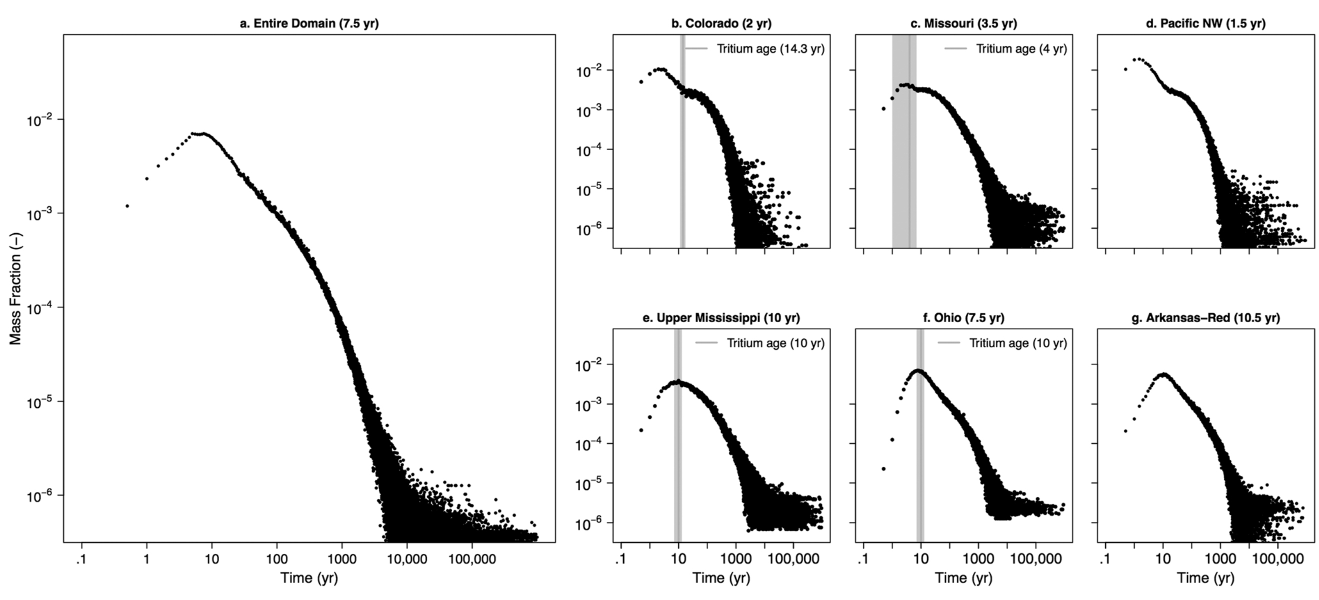

Figure 2. The distribution of groundwater residence times is shown to agree with the inferred tritium ages and to provide understanding of the wide range of residence times calculated for the entire domain and each watershed. Log-log plots of flux-weighted mass fraction (the fraction of water in a basin of a given residence time) are shown here as a function of residence time for (a) the entire domain and (b–g) major North American river basins. The peak (maximum) arrival time is indicated in each subfigure title and the inferred tritium ages are indicated on four basins as shown (as summarized in *Stewart et al*. [2010]).

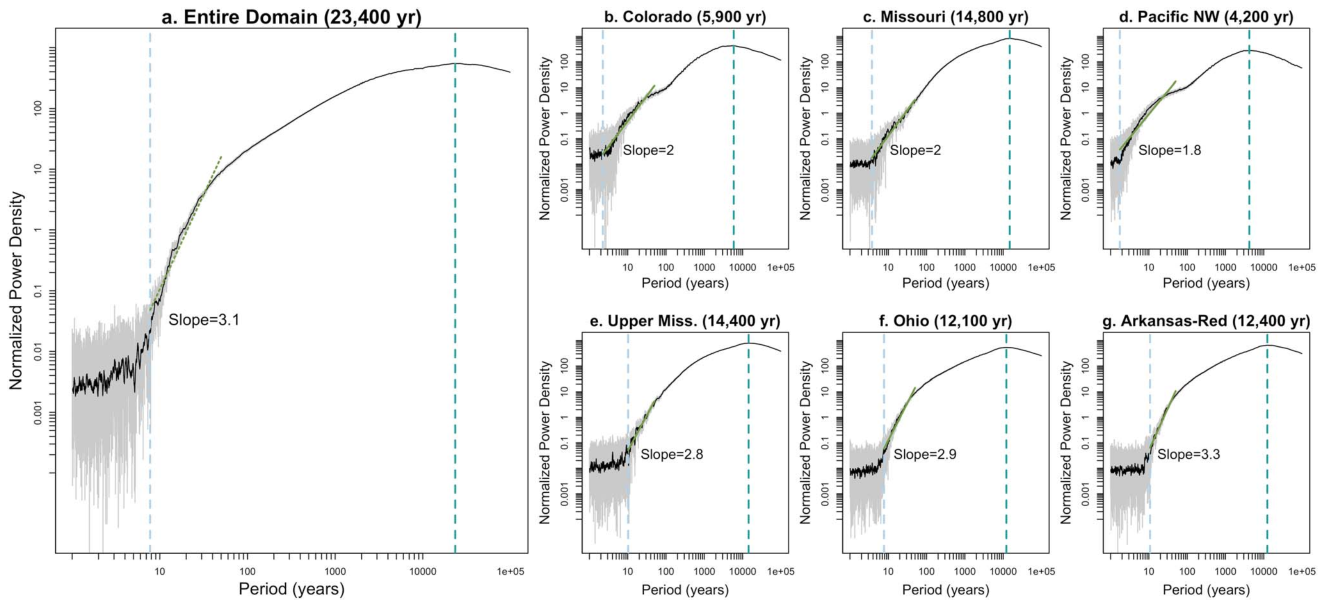

Figure 3. Periodograms of the residence time distributions show a range of behavior depending on period. (a) The entire domain and all major basins (b–g) all show white noise at earlier times (less than 10 years as indicated by the first blue line in each panel) and are unorganized at late times (past 10,000 years as indicated by the second blue line in each panel and given in the panel caption). Between 10 and 10,000 years a range of behaviors is seen, as indicated by the initial slope of the log spectra, also indicated on each panel. Note the black curve is smoothed from the raw spectra (in gray) for plotting purposes.

connected through the control that K exerts on water table depth [see *Maxwell et al.*, 2015, Figure 9]. Additionally, we see that the three basins with the lowest peak age are western rivers that gain much of their flow from higher elevations where, as discussed earlier, residence times are shorter. The semivariance of simulated age is also shown to be a function of aridity (Figure 4b) when the basin-averaged semivariance of ln(age) (a measure of the slope and spread in Figures 2b–2g) is plotted as a function of modeled *P-ET* (the precipitation minus evapotranspiration used to drive the flow model). The more subtle physical mechanisms that we hypothesize control this relationship are explored conceptually in Figure 5. In this figure, more humid basins (with greater *P-ET*) typically have shallower water tables that more closely follow topography, including more intersections with the ground surface, more local flow paths and thus more stagnation points. Topography is fractal [*Rodriguez-Iturbe and Rinaldo*, 2001] both in real systems and in our domain and locations where the water table follows topography will have different age distributions as seen by the larger semivariances. More arid basins (with lower *P-ET*) tend to have deeper water tables that are flatter and less likely to follow

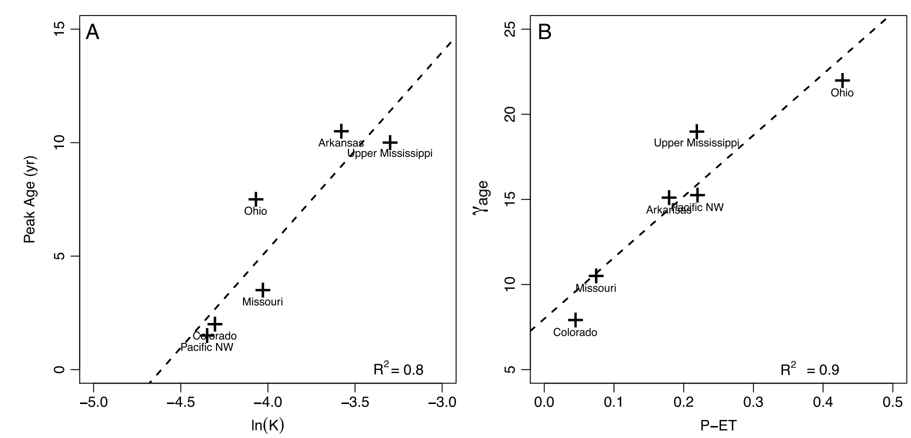

Figure 4. Peak age is a function of geology, whereas the age distribution is a function of aridity. These scatterplots show correlations between the (a) peak residence time versus the geometric mean of hydraulic conductivity and (b) semivariance of natural log residence time (γ_{age}) versus the average *P-ET* for each of the continental basins in this study.

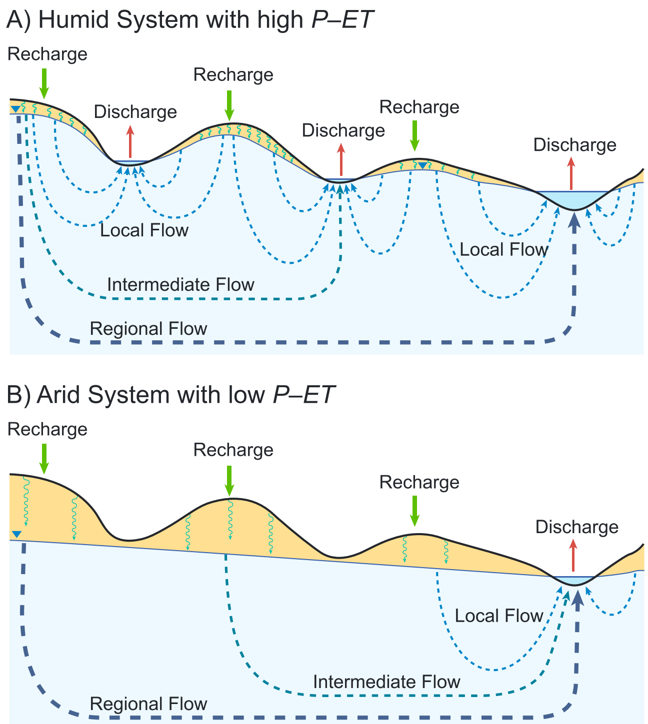

Figure 5. This conceptual diagram of the influence of aridity on age distributions demonstrates how aridity decreases the variance of the distribution of ages. For the humid system (a) the water table is shallower, is heavily influenced by topography, and has more discharge points. For the arid system (b) the water table is deeper, flatter, less influenced by topography and has fewer discharge points. Diagram modified and combined from several prior studies [*Tóth*, 1963; *Haitjema and Mitchell-Bruker*, 2005; *Gleeson and Manning*, 2008; *Schaller and Fan*, 2009].

topography, resulting in subsequently smaller semivariances. Note that many other relationships were explored (e.g., semivariance of age versus average of ln(K)) but showed no correlation. This possible explanation for reduced semivariance of the residence time distribution could oversimplify more complex recharge patterns that occur in mountain-block systems (such as the Colorado and Snake watersheds, which as discussed previously exhibit a bimodal distribution of age) and the scale and extent of these relationships should be explored further.

The effect of spatial resolution on model results is evaluated by comparing to a recent modeling study of a mountain headwaters system that used a similar modeling approach but at a higher (20 m) spatial resolution [*Engdahl and Maxwell*, 2015]. *Engdahl and Maxwell* [2015] found changes in *P-ET* yielded nonuniform changes in water table depth, altering the distribution of age due to the proportion of time spent in unsaturated and saturated regions. The finer resolution model of *Engdahl and Maxwell* [2015] contained less than 4% of water ages one year or less (i.e., roughly the lower limit of the ages seen in larger scale/coarser resolution model). This suggests that resolutions less than 1 km are needed to accurately capture some of these early times. However, agreement is seen between the age distributions predicted by both models (see Figure S1). The age ranges found in both studies also bracket ranges inferred for another headwaters system from radioisotopes [*Manning and Caine*, 2007] as well as connections between recharge, water table depth, and age [*Manning et al.*, 2013].

Our work demonstrates the feasibility of using integrated hydrologic models to directly simulate water age. These findings suggest a connection between theoretical studies driven purely by topography [*Wörman et al.*, 2007] with observations of path length and related parameters [*McGuire et al.*, 2005] and suggest that both K and *P-ET* contribute to effective age. We have compared our model results with available, large-scale observational data; however, these data are quite limited and much additional study is needed to confirm the correlations suggested here.

4. Conclusions

Long-standing conceptual models of large-scale water table behavior [*Tóth*, 1963; *Haitjema and Mitchell-Bruker*, 2005; *Gleeson and Manning*, 2008] are linked to water residence time through fundamental drivers, further connecting climate and land cover alterations to water quality [*Aubert et al.*, 2013; *Bearup et al.*, 2014]. The continental-scale residence time simulations presented here indicate that stream water ages for major river basins may have power-law distributions with peaks from 1.5 to 10.5 years and a mix of very old and very young water. Additionally, our results suggest that the peak groundwater ages may be driven by hydraulic conductivity whereas the semivariance of the distribution is a function of aridity. These findings reinforce the importance of comprehensive observations of high-frequency measurements of stream compositions both to determine age of water [*Stewart et al*., 2012] and to better infer fundamental basin properties such as potential recharge, permeability, and porosity. Results further underscore the need for a holistic understanding of the connected hydrologic cycle, particularly for projecting large-scale water quality impacts that may persist given the large quantities of old water contributing to tributary groundwater.

Acknowledgments
All numerical results from this work are available upon request. This work was supported by the National Science Foundation grants WSC-1204787 and DGE-1069333, and by the US Department of Energy Office of Science, Offices of Advanced Scientific Computing Research (ASCR) and Biological Environmental Sciences (BER). The authors wish to thank the Editor, Associate Editor, two anonymous reviewers, and T. Gleeson for their comments contributing to the clarity and quality of this work.

References

Aubert, A. H., J. W. Kirchner, C. Gascuel-Odoux, M. Faucheux, G. Gruau, and P. Merot (2013), Fractal water quality fluctuations spanning the periodic table in an intensively farmed watershed, *Environ. Sci. Technol.*, *48*(2), 930–937.

Bearup, L. A., R. M. Maxwell, D. W. Clow, and J. E. McCray (2014), Hydrological effects of forest transpiration loss in bark beetle-impacted watersheds, *Nat. Clim. Change*, *4*(6), 481–486.

Botter, G., E. Bertuzzo, and A. Rinaldo (2010), Transport in the hydrologic response: Travel time distributions, soil moisture dynamics, and the old water paradox, *Water Resour. Res.*, *46*, W03514, doi:10.1029/2009WR008371.

Cardenas, M. B. (2007), Potential contribution of topography-driven regional groundwater flow to fractal stream chemistry: Residence time distribution analysis of Toth flow, *Geophys. Res. Lett.*, *34*, L05403, doi:10.1029/2006GL029126.

Cardenas, M. B. I. (2008), Surface water-groundwater interface geomorphology leads to scaling of residence times, *Geophys. Res. Lett.*, *35*, L08402, doi:10.1029/2008GL033753.

Cardenas, M. B., J. L. Wilson, and R. Haggerty (2008), Residence time of bedform-driven hyporheic exchange, *Adv. Water Resour.*, *31*(10), 1382–1386.

Engdahl, N. B., and R. M. Maxwell (2015), Quantifying changes in age distributions and the hydrologic balance of a high-mountain watershed from climate induced variations in recharge, *J. Hydrol.*, *522*, 152–162.

Fan, Y., G. Miguez-Macho, C. P. Weaver, R. Walko, and A. Robock (2007), Incorporating water table dynamics in climate modeling: 1. Water table observations and equilibrium water table simulations, *J. Geophys. Res.*, *112*, D10125, doi:10.1029/2006JD008111.

Fiori, A., and D. Russo (2008), Travel time distribution in a hillslope: Insight from numerical simulations, *Water Resour. Res.*, *44*, W12426, doi:10.1029/2008WR007135.

Flewelling, S. A., J. S. Herman, G. M. Hornberger, and A. L. Mills (2012), Travel time controls the magnitude of nitrate discharge in groundwater bypassing the riparian zone to a stream on Virginia's coastal plain, *Hydrol. Processes*, *26*, 1242–1253.

Frisbee, M. D., J. L. Wilson, J. D. Gomez-Velez, F. M. Phillips, and A. R. Campbell (2013), Are we missing the tail (and the tale) of residence time distributions in watersheds?, *Geophys. Res. Lett.*, *40*, 4633–4637, doi:10.1002/grl.50895.

Gleeson, T., and A. H. Manning (2008), Regional groundwater flow in mountainous terrain: Three-dimensional simulations of topographic and hydrogeologic controls, *Water Resour. Res.*, *44*, W10403, doi:10.1029/2008WR006848.

Gleeson, T., L. Smith, N. Moosdorf, J. Hartmann, H. H. Dürr, A. H. Manning, L. P. H. van Beek and A. M. Jellinek (2011), Mapping permeability over the surface of the Earth, *Geophys. Res. Lett.*, *38*, L02401, doi:10.1029/2010GL045565.

Haggerty, R., S. M. Wondzell and M. A. Johnson (2002), Power-law residence time distribution in the hyporheic zone of a 2nd-order mountain stream, *Geophys. Res. Lett.*, *29*(13), 1640, doi:10.1029/2002GL014743.

Haitjema, H. M., and S. Mitchell-Bruker (2005), Are water tables a subdued replica of the topography?, *Ground Water*, *43*(6), 781–786.

Hrachowitz, M., H. Savenije, T. A. Bogaard, D. Tetzlaff, and C. Soulsby (2013), What can flux tracking teach us about water age distribution patterns and their temporal dynamics?, *Hydrol. Earth Syst. Sci.*, *17*(2), 533–564.

Jiang, X. W., L. Wan, M. B. Cardenas, S. Ge, and X.-S. Wang (2010), Simultaneous rejuvenation and aging of groundwater in basins due to depth-decaying hydraulic conductivity and porosity, *Geophys. Res. Lett.*, *37*, L05403, doi:10.1029/2010GL042387.

Kirchner, J. W. (2003), A double paradox in catchment hydrology and geochemistry, *Hydrol. Processes*, *17*(4), 871–874.

Kirchner, J. W., and C. Neal (2013), Universal fractal scaling in stream chemistry and its implications for solute transport and water quality trend detection, *Proc. Natl. Acad. Sci. U.S.A.*, *110*(30), 12,213–12,218.

Kirchner, J. W., X. H. Feng, and C. Neal (2000), Fractal stream chemistry and its implications for contaminant transport in catchments, *Nature*, *403*(6769), 524–527.

Kollet, S. J., and R. M. Maxwell (2008), Demonstrating fractal scaling of baseflow residence time distributions using a fully-coupled groundwater and land surface model, *Geophys. Res. Lett.*, *35*, L07402, doi:10.1029/2008GL033215.

Laudon, H., M. Berggren, A. Agren, I. Buffam, K. Bishop, T. Grabs, M. Jansson, and S. Kohler (2011), Patterns and dynamics of dissolved organic carbon (DOC) in boreal streams: The role of processes, connectivity, and scaling, *Ecosystems*, *14*, 880–893.

Maher, K., and C. P. Chamberlain (2014), Hydrologic regulation of chemical weathering and the geologic carbon cycle, *Science*, *343*(6178), 1502–1504.

Manning, A. H., and J. S. Caine (2007), Groundwater noble gas, age, and temperature signatures in an Alpine watershed: Valuable tools in conceptual model development, *Water Resour. Res.*, *43*, W04404, doi:10.1029/2006WR005349.

Manning, A. H., P. L. Verplanck, J. S. Caine, and A. S. Todd (2013), Links between climate change, water-table depth, and water chemistry in a mineralized mountain watershed, *Appl. Geochem.*, *13*, 64–78.

Maxwell, R. M., L. E. Condon, and S. J. Kollet (2015), A high-resolution simulation of groundwater and surface water over most of the continental US with the integrated hydrologic model ParFlow v3, *Geosci. Model Dev.*, *8*, 1–15.

McDonnell, J. J., et al. (2010), How old is streamwater? Open questions in catchment transit time conceptualization, modelling and analysis, *Hydrol. Processes*, *24*(12), 1745–1754.

McGuire, K. J., J. J. McDonnell, M. Weiler, C. Kendall, B. L. McGlynn, J. M. Welker, and J. Seibert (2005), The role of topography on catchment-scale water residence time, *Water Resour. Res.*, *41*, W05002, doi:10.1029/2004WR003657.

Montgomery, D. R., and W. E. Dietrich (1992), Channel Initiation and the Problem of Landscape Scale, *Science*, *255*(5046), 826–830.

Quinodoz, H. A. M., and A. J. Valocchi (1993), Stochastic-analysis of the transport of kinetically sorbing solutes in aquifers with randomly heterogeneous hydraulic conductivity, *Water Resour. Res.*, *29*, 3227–3240, doi:10.1029/93WR01039.

Rinaldo, A., K. J. Beven, E. Bertuzzo, L. Nicotina, J. Davies, A. Fiori, D. Russo, and G. Botter (2011), Catchment travel time distributions and water flow in soils, *Water Resour. Res.*, *47*, W07537, doi:10.1029/2011WR010478.

Rodriguez-Iturbe, I., and A. Rinaldo (2001), *Fractal river basins: Chance and self-organization*, Cambridge Univ. Press, Cambridge, U. K.

Schaap, M. G., and F. J. Leij (1998), Database-related accuracy and uncertainty of pedotransfer functions, *Soil Sci.*, *163*(10), 765–779.

Schaller, M. F., and Y. Fan (2009), River basins as groundwater exporters and importers: Implications for water cycle and climate modeling, *J. Geophys. Res.*, *114*, D04103, doi:10.1029/2008JD010636.

Scher, H., G. Margolin, R. Metzler, J. Klafter and B. Berkowitz (2002), The dynamical foundation of fractal stream chemistry: The origin of extremely long retention times, *Geophys. Res. Lett.*, *29*(5), 1061, doi:10.1029/2001GL014123.

Sposito, G., and W. A. Jury (1988), The lifetime probability density-function for solute movement in the subsurface zone, *J. Hydrol.*, *102*, 503–518.

Stewart, M. K., U. Morgenstern, and J. J. McDonnell (2010), Truncation of stream residence time: How the use of stable isotopes has skewed our concept of streamwater age and origin, *Hydrol. Processes*, *24*(12), 1646–1659.

Stewart, M. K., U. Morgenstern, J. J. McDonnell, and L. Pfister (2012), The 'hidden streamflow' challenge in catchment hydrology: A call to action for stream water transit time analysis, *Hydrol. Processes*, *26*(13), 2061–2066.

Stonedahl, S. H., J. W. Harvey, J. Detty, A. Aubeneau, and A. I. Packman (2012), Physical controls and predictability of stream hyporheic flow evaluated with a multiscale model, *Water Resour. Res.*, *48*, W10513, doi:10.1029/2011WR011582.

Tetzlaff, D., J. Seibert, K. J. McGuire, H. Laudon, D. A. Burns, S. M. Dunn, and C. Soulsby (2009), How does landscape structure influence catchment transit time across different geomorphic provinces?, *Hydrol. Processes*, *23*(6), 945–953.

Tóth, J. (1963), A theoretical analysis of groundwater flow in small drainage basins, *J. Geophys. Res.*, *68*(16), 4795–4812, doi:10.1029/JZ068i016p04795.

Wörman, A., A. I. Packman, L. Marklund, J. W. Harvey and S. H. Stone (2007), Fractal topography and subsurface water flows from fluvial bedforms to the continental shield, *Geophys. Res. Lett.*, *34*, L07402, doi:10.1029/2007GL029426.